

Lead isotope signatures of Tintina Gold Province intrusions and associated mineral deposits from southeastern Yukon and southwestern Northwest Territories: Implications for exploration in the southeastern Tintina Gold Province

R. Scott Heffernan¹
Equity Engineering Ltd.

James K. Mortensen² and Janet E. Gabites³
Pacific Centre for Isotopic and Geochemical Research at the University of British Columbia

V. Sterenberg
Department of Indian and Northern Affairs, Government of the Northwest Territories⁴

Heffernan, R.S., Mortensen, J.K., Gabites, J.E. and Sterenberg, V., 2005. Lead isotope signatures of Tintina Gold Province intrusions and associated mineral deposits from southeastern Yukon and southwestern Northwest Territories: Implications for exploration in the southeastern Tintina Gold Province. *In: Yukon Exploration and Geology 2004*, D.S. Emond, L.L. Lewis and G.D. Bradshaw (eds.), Yukon Geological Survey, p. 121-128.

ABSTRACT

This paper presents new lead isotope data from intrusive rocks and several mineral deposits from the southeastern portion of the Tintina Gold Province (TGP). Lead isotopic studies of feldspars separated from various mid-Cretaceous intrusions in the study area and sulphide minerals from a number of mineral occurrences that are spatially associated with the intrusions were done in order to investigate possible relationships between the mineralization and magmatism. These data provide insight on metal sources within these systems and hence help to constrain exploration models. Results from this study indicate that: 1) the metals in many mineral deposits and prospects in the region are mostly derived from the mid-Cretaceous TGP intrusions; 2) the Sa Dena Hes deposit is broadly mid-Cretaceous in age; and 3) metals in apparently distal styles of intrusion-related gold mineralization are not entirely derived from magmatic sources.

RÉSUMÉ

Nous présentons de nouvelles données sur les isotopes du plomb dans les roches intrusives et plusieurs gîtes minéraux dans la partie sud-est de la province aurifère de Tintina (PAT). Pour étudier les relations possibles entre la minéralisation et le magmatisme, nous avons aussi analysé les isotopes du plomb dans des feldspaths séparés de diverses intrusions datant du Crétacé moyen dans l'aire d'étude, ainsi que dans des minéraux sulfurés provenant d'un certain nombre d'occurrences minéralisées associées aux intrusions. Ces données renseignent sur les sources de métaux dans ces systèmes et permettent ainsi d'imposer des limites aux modèles d'exploration. Les résultats de cette étude indiquent 1) que les métaux présents dans de nombreux gîtes (et occurrences) minéraux de la région proviennent surtout d'intrusions du Crétacé moyen dans la PAT, 2) que le gîte Sa Dena Hes remonte à peu près au Crétacé moyen, et 3) que les métaux présents dans des types apparemment distaux de minéralisations en or liées aux intrusions ne proviennent pas entièrement de sources magmatiques.

¹scotth@equityeng.bc.ca

²jmortensen@eos.ubc.ca

³gabites@eos.ubc.ca

⁴Yellowknife, Northwest Territories, Canada

INTRODUCTION

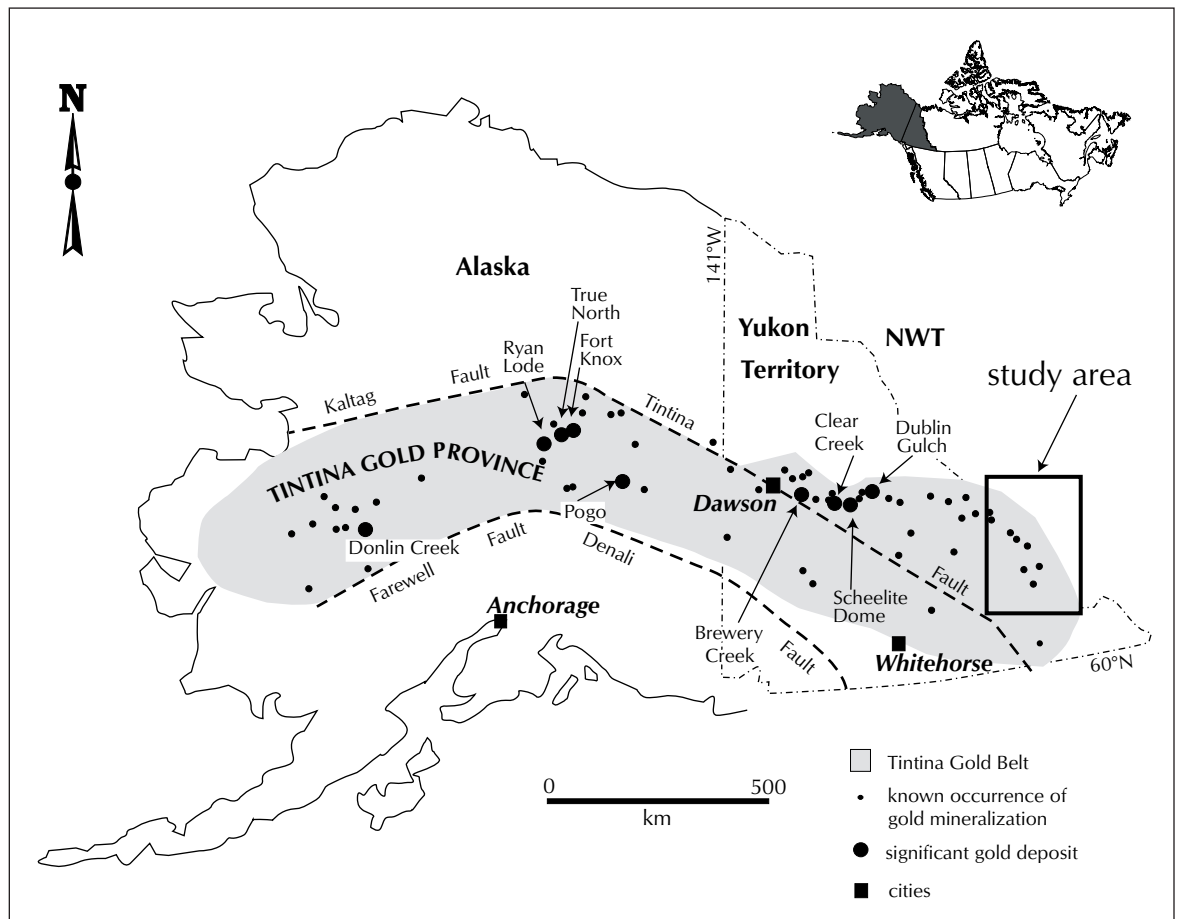
The Tintina Gold Province (TGP) in east-central Alaska, Yukon Territory, and southwestern Northwest Territories is host to numerous styles of precious- and base-metal mineralization thought to be genetically associated with widespread Early to Late Cretaceous magmatism (Fig. 1). Styles of mineralization in the TGP are highly variable and include sheeted quartz-feldspar veins, polymetallic replacement bodies, auriferous breccias, disseminated mineralization, gold-rich skarns, and epithermal vein systems (especially associated with Late Cretaceous intrusive and volcanic rocks). In the early 1990s, the discovery of gold deposits such as Fort Knox and Brewery Creek spurred exploration activity which led to further discoveries at Pogo, Donlin Creek, True North, Dublin Gulch, Ryan Lode, and Scheelite Dome. The rush of exploration success was accompanied by significant research directed at the development of genetic and exploration models. The resulting "Intrusion-Related Gold Systems" (IRGS) model has been continuously evolving since its inception (Thompson et al., 1999; Lang, 2000; Hart et al, 2000; Lang and Baker, 2001).

This paper presents new lead isotope data from intrusive rocks and several mineral deposits from the southeastern portion of the TGP. These data help to constrain metal sources within these systems and hence provide insight into possible relationships between magmatism and mineralization. The results of this study will help to refine exploration models that target mineralization in this region.

REGIONAL METALLOGENY

A variety of intrusion-hosted and (probably) intrusion-related deposits and occurrences are known in the eastern Selwyn Basin, including tungsten (\pm base metal) skarns such as Mactung, Cantung and Lened, silver-rich base metal skarns and mantos such as Sa Dena Hes, gold-bearing sheeted quartz-feldspar veins (e.g., within the Mactung intrusion), distal, apparently structurally controlled deposits such as Hyland, and massive sulphide replacement deposits such as Quartz Lake (McMillan; Fig. 2). Indeed, at least 45% of the 325 MINFILE occurrences (Deklerk and Traynor, 2004) listed for the six

Figure 1. Map of Alaska State and Yukon Territory showing the extent of the Tintina Gold Province and significant gold deposits and occurrences within (after Mortensen et al., 2000). The main study area is outlined at right.



map sheets that compose the study area (105-A, -H, -I, and 95-D, -E, -L) are definitely or arguably intrusion-related. A discussion on the mineral potential of the eastern Selwyn Basin would not be complete without mention of the numerous sedimentary-exhalative (SEDEX)-type occurrences such as the Howard's Pass deposit and the Matt Berry prospect. The combination of both syngenetic and epigenetic exploration targets has led to a considerable amount of interest from exploration companies in the mineral potential of this region in the past several decades.

GEOLOGIC OVERVIEW

One of the most striking features of the southeastern TGP is the great volume of granitic intrusions present; more than 5000 km² of mid-Cretaceous intrusive rocks are exposed within the study area (Fig. 2). These intrusions

consist of simple to complex, single- to multi-phase stocks, plutons and batholiths. Major intrusive phases consist mainly of medium-grained, massive to megacrystic granodiorite, quartz monzonite and granite. Intrusions of the southeastern TGP were emplaced into Late Precambrian to Mesozoic strata of the Selwyn Basin. Stratigraphy of the Selwyn Basin in this region consists mainly of turbiditic sandstone, deep water limestone, shale and chert that were deposited contemporaneously with shallow water carbonate and sandstone of the Mackenzie platform to the north and east (Gordey and Anderson, 1993). Results of geochronological, geochemical and isotopic investigations (Heffernan, 2004) indicate that the known plutonic suites of the western and northern portions of the TGP (Mortensen et al., 2000) do continue into southeastern Yukon and southwestern Northwest Territories.

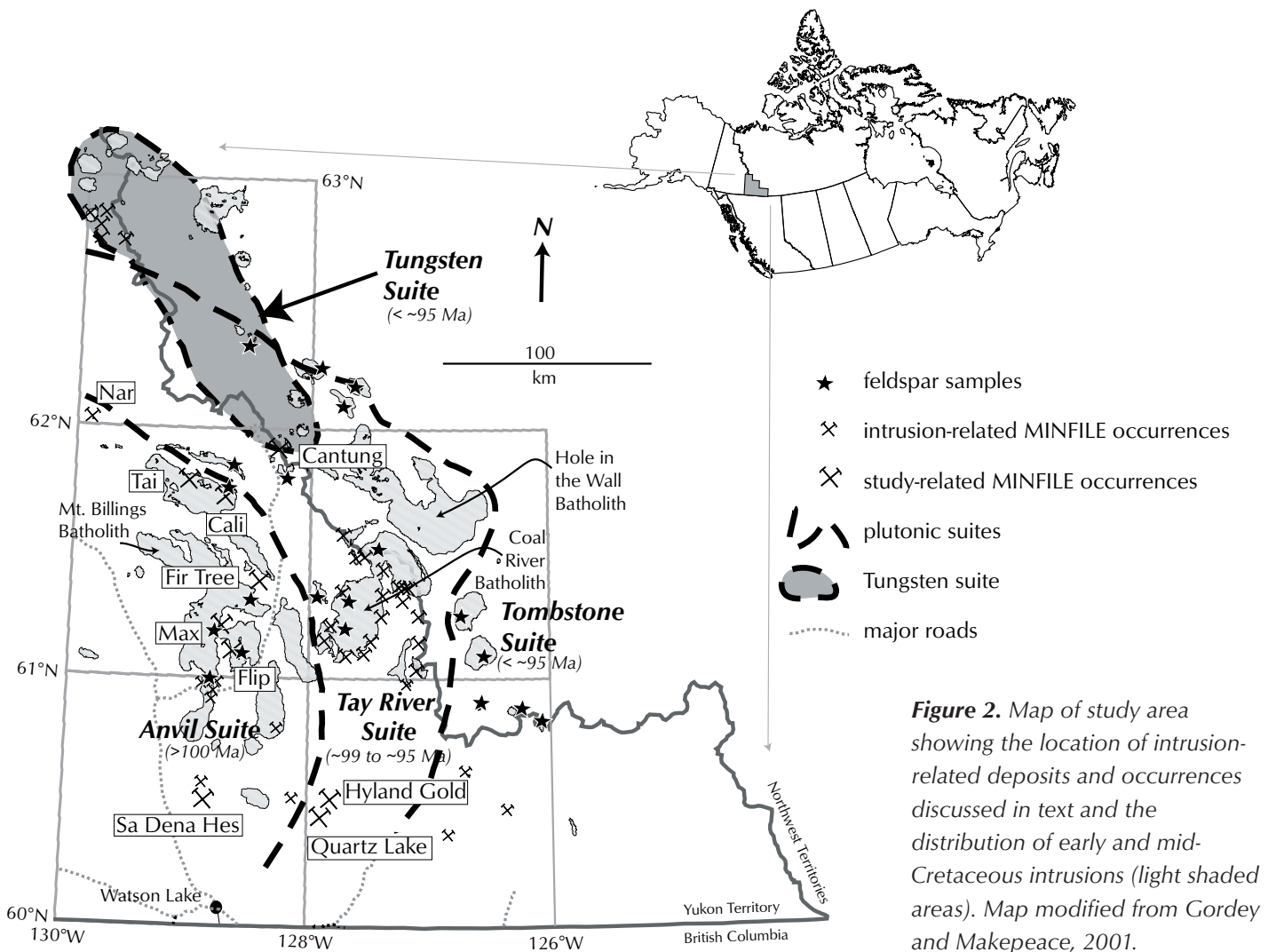


Figure 2. Map of study area showing the location of intrusion-related deposits and occurrences discussed in text and the distribution of early and mid-Cretaceous intrusions (light shaded areas). Map modified from Gordey and Makepeace, 2001.

LEAD ISOTOPE STUDY

Pb isotope studies of feldspars separated from various mid-Cretaceous intrusions in the study area and of sulphide minerals from a number of precious- and base-metal deposits and occurrences have been carried out in order to investigate possible genetic relationships between mineralization and magmatism.

SAMPLES AND ANALYTICAL TECHNIQUES

Sulphide samples were collected from numerous mineral deposits and occurrences that were examined during the course of this study. Names and brief descriptions of the sampled occurrences are presented in Table 1, and sample locations are shown in Figure 2. All sample preparation, geochemical separations and isotopic measurements were done at Pacific Centre for Isotopic and Geochemical Research (PCIGR) at the University of British Columbia. Additional discussion of the samples and the analytical techniques that were employed is presented in Heffernan (2004). For trace lead sulphide samples, approximately 10 to 50 milligrams of hand-picked sulphide minerals were first leached in dilute hydrochloric acid to remove surface contamination and then dissolved in dilute nitric acid. Samples of galena required no leaching and were directly dissolved in dilute hydrochloric acid. Following ion exchange chemistry, approximately 10 to 25 nanograms of lead in chloride form was loaded on rhenium filaments using a phosphoric acid-silica gel emitter. Isotopic ratios were determined with a modified VG54R thermal ionization mass spectrometer in peak-switching mode on a Faraday detector. Measured ratios were corrected for instrumental mass fractionation of 0.12%/amu based on repeated measurements of the NBS 981 standard and the values

recommended by Thirwall (2000). Errors were numerically propagated throughout all calculations and are reported at the 2σ level (Table 2).

RESULTS

The results from Pb isotope analyses of feldspar and sulphide mineral separates are presented in Table 2 and are plotted in Figure 3 with reference to the upper-crustal Pb evolution model (Shale Curve) of Godwin and Sinclair (1982). The Shale Curve is of particular relevance to this study as it is based on the Pb isotope compositions of shale-hosted lead-zinc deposits located within the Canadian Cordillera miogeocline. The new data are plotted together with previously determined lead isotopic compositions for other sulphide occurrences in the area (discussed later).

Lead isotopic analyses of feldspar collected from intrusions throughout the region generally yield quite consistent lead isotopic compositions (Table 2) with the exception of one sample (SH-011E-INT) collected from the Mt. Billings occurrence, which returned significantly more radiogenic values. With that single exception, the lead isotopic compositions ($n=19$) show little variation in $^{206}\text{Pb}/^{204}\text{Pb}$, $^{207}\text{Pb}/^{204}\text{Pb}$, $^{208}\text{Pb}/^{204}\text{Pb}$, $^{207}\text{Pb}/^{206}\text{Pb}$ and $^{208}\text{Pb}/^{206}\text{Pb}$ ratios, with narrow ranges of 19.397 to 19.651, 15.697 to 15.829, 39.461 to 39.883, 0.805 to 0.811 and 2.020 to 2.037, respectively.

Lead isotopic analyses for sulphide samples from mineral occurrences that are spatially associated with the intrusions also generally yield similar lead isotopic compositions (Table 2). Exceptions include three samples (SH-073-1, SH-070-1 and -2) from the Tai and Cali mineral occurrences at the north end of the Mt. Billings Batholith (Fig. 2), which returned the least radiogenic $^{207}\text{Pb}/^{206}\text{Pb}$

Table 1. Location and basic descriptions of deposits and occurrences examined during this study.

Occurrence/ deposit	MINFILE reference	Commodities	Location		Status	Samples
			Northing	Easting		
Tai	105H 073	W, Cu, Zn, Mo	6854191	497966	drilled prospect	SH-073-1, SH-073-2
Cali	105H 070	W, Cu, Ag	6845327	518253	drilled prospect	SH-070, SH-070s
Flip	105H 005	Ag, Pb, Zn, W, Cu	6778677	518322	prospect	SH-005-1
Max	105H 011	Pb, Zn, Ag, W, Cu	6795031	515542	drilled prospect	SH-011E-1 to -4
Fir Tree	105H 029	Pb, Zn, Ag, Cu, W	6808645	529674	drilled prospect	SH-028-1, SH-029-2
Sa Dena Hes (Mt. Hundere)	105A 012	Zn, Pb, Ag	6709115	506817	past underground producer	SH-SDH (this study), 10138-001, -002, 501

Table 2. Pb isotope data from feldspar and sulphide mineral separates analysed during this study. All analyses were conducted in the Pacific Centre for Isotopic and Geochemical Research at the University of British Columbia. Mineral abbreviations: fs – feldspar; po – pyrrhotite; gl – galena; cp – chalcopyrite; py – pyrite. Samples SH-HY-01 to 04 are from the Hyland Au occurrence (Fig. 2) and were provided to the primary author by StrataGold Corp. Italicized samples are from intrusions and not necessarily associated with a specific mineral occurrence. Locations are shown as stars on Figure 2.

Sample	Source	Mineral	²⁰⁶ Pb/ ²⁰⁴ Pb	2σ,%	²⁰⁷ Pb/ ²⁰⁴ Pb	2σ,%	²⁰⁸ Pb/ ²⁰⁴ Pb	2σ,%	²⁰⁷ Pb/ ²⁰⁶ Pb	2σ,%	²⁰⁸ Pb/ ²⁰⁶ Pb	2σ,%
<i>98-HAS-02</i>	Mt. Appler pluton	fs	19.490	0.03	15.757	0.04	39.541	0.06	0.80844	0.02	2.02878	0.03
<i>98-HAS-03</i>	Faille pluton	fs	19.440	0.03	15.731	0.04	39.480	0.06	0.80920	0.02	2.03090	0.03
<i>98-HAS-06</i>	Mulholland (Cirque) pluton	fs	19.487	0.04	15.751	0.05	39.578	0.07	0.80830	0.02	2.03103	0.04
<i>98-HAS-07</i>	Jorgensen pluton	fs	19.560	0.04	15.754	0.05	39.673	0.07	0.80541	0.02	2.02830	0.03
<i>98-HAS-12</i>	Patterson pluton	fs	19.534	0.08	15.771	0.08	39.757	0.10	0.80736	0.04	2.03530	0.04
<i>98-HAS-14</i>	McLeod pluton	fs	19.594	0.03	15.772	0.05	39.577	0.06	0.80496	0.02	2.01991	0.03
<i>98-Z-12</i>	Powers pluton	fs	19.651	0.11	15.829	0.12	39.883	0.13	0.80553	0.02	2.02960	0.03
<i>98-Z-C028</i>	Rudi Pluton	fs	19.493	0.03	15.750	0.05	39.569	0.06	0.80797	0.02	2.02993	0.03
<i>99SH-001</i>	Shannon Creek pluton	fs	19.404	0.03	15.732	0.04	39.461	0.06	0.81076	0.02	2.03365	0.03
<i>99SH-006</i>	Coal River Batholith	fs	19.477	0.10	15.771	0.10	39.640	0.11	0.80975	0.02	2.03526	0.03
<i>99SH-008</i>	Coal River Batholith	fs	19.460	0.09	15.741	0.09	39.596	0.10	0.80893	0.02	2.03480	0.03
<i>99SH-011</i>	Big Charlie pluton	fs	19.585	0.03	15.788	0.04	39.618	0.06	0.80612	0.02	2.02294	0.03
<i>99SH-023</i>	Mt. Billings Batholith	fs	19.447	0.04	15.749	0.05	39.598	0.07	0.80983	0.02	2.03621	0.04
<i>SH-005-INT</i>	Mt. Billings Batholith	fs	19.447	0.24	15.697	0.24	39.528	0.25	0.80718	0.05	2.03259	0.05
<i>SH-073-INT</i>	Mt. Billings Batholith	fs	19.473	0.03	15.762	0.05	39.591	0.06	0.80943	0.02	2.03317	0.03
<i>99SH-009</i>	Coal River Batholith	fs	19.545	0.04	15.757	0.05	39.670	0.07	0.80621	0.02	2.02969	0.03
<i>99SH-013</i>	Caesar Lakes pluton	fs	19.397	0.03	15.713	0.05	39.469	0.07	0.81007	0.02	2.03484	0.03
<i>99SH-016</i>	Tuna Stock	fs	19.530	0.04	15.798	0.05	39.774	0.07	0.80890	0.03	2.03658	0.04
<i>SH-011E-INT</i>	Mt. Billings Batholith	fs	19.772	0.04	15.810	0.05	39.786	0.07	0.79962	0.02	2.01221	0.03
<i>SH-029-INT</i>	Mt. Billings Batholith	fs	19.444	0.03	15.730	0.05	39.467	0.07	0.80899	0.02	2.02983	0.03
<i>SH-005-1</i>	Flip	po	19.579	0.05	15.775	0.06	39.750	0.07	0.80569	0.02	2.03022	0.03
<i>SH-011E-1</i>	Max	gl	19.473	0.03	15.731	0.04	39.482	0.06	0.80787	0.02	2.02757	0.03
<i>SH-011E-2</i>	Max	gl	19.491	0.03	15.752	0.05	39.545	0.06	0.80817	0.02	2.02888	0.03
<i>SH-011E-3</i>	Max	cp	19.615	0.04	15.904	0.05	40.039	0.07	0.81080	0.02	2.04126	0.03
<i>SH-011E-4</i>	Max	py	19.494	0.03	15.758	0.05	39.594	0.07	0.80832	0.02	2.03107	0.03
<i>SH-029-1</i>	Fir Tree	gl	19.396	0.04	15.728	0.05	39.445	0.07	0.81092	0.02	2.03373	0.03
<i>SH-029-2</i>	Fir Tree	po	19.467	0.03	15.795	0.05	39.709	0.06	0.81136	0.02	2.03979	0.03
<i>SH-070</i>	Cali	po	20.550	0.05	15.702	0.05	40.003	0.07	0.76406	0.03	1.94663	0.04
<i>SH-070s</i>	Cali	po	21.106	0.15	15.843	0.21	42.657	0.28	0.75066	0.07	2.02121	0.14
<i>SH-073-1</i>	Tai	po	19.915	0.15	15.797	0.21	39.648	0.28	0.79325	0.07	1.99101	0.14
<i>SH-073-2</i>	Tai	po	19.513	0.10	15.780	0.11	39.500	0.12	0.80873	0.02	2.02436	0.03
<i>SH-SDH</i>	Sa Dena Hes	gl	19.397	0.03	15.711	0.05	39.391	0.07	0.80998	0.02	2.03081	0.04
<i>SH-HY-01</i>	Hyland	py	20.066	0.11	15.779	0.10	40.174	0.06	0.78640	0.08	2.00210	0.06
<i>SH-HY-02</i>	Hyland	py	20.182	0.05	15.807	0.07	40.167	0.04	0.78320	0.03	1.99020	0.05
<i>SH-HY-03</i>	Hyland	py	20.236	0.05	15.871	0.07	40.391	0.04	0.78430	0.03	1.99600	0.04
<i>SH-HY-04</i>	Hyland	py	20.475	0.05	15.889	0.07	40.366	0.04	0.77600	0.02	1.97150	0.05

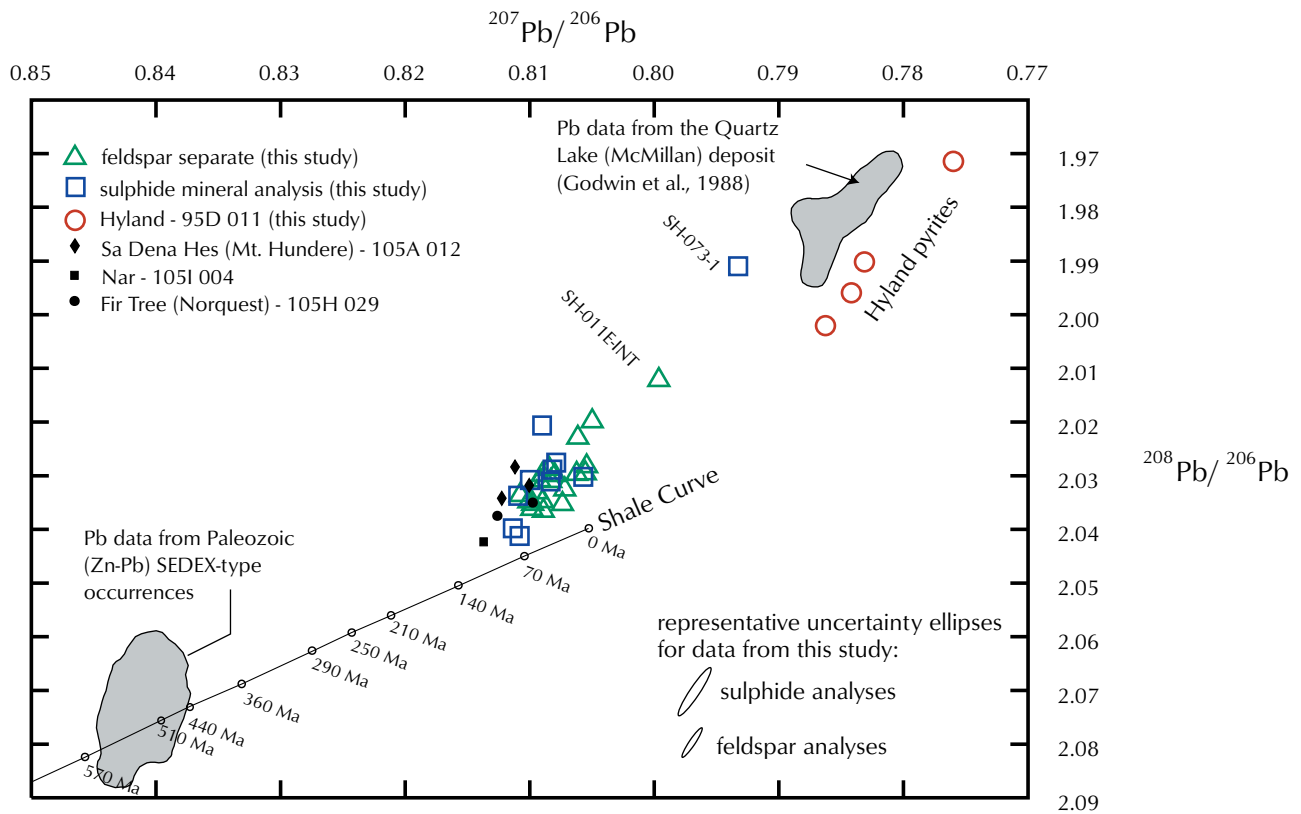


Figure 3. $^{207}\text{Pb}/^{206}\text{Pb}$ versus $^{208}\text{Pb}/^{206}\text{Pb}$ plot of Pb data from this study and similar data compiled from Godwin et al. (1988) for other mineral occurrences and deposits from within the study area (see text for discussion). Lead data for the Paleozoic SEDEX-type occurrences includes data from the Howard's Pass, Matt Berry, Mel-Hoser, Maxi, and Pas occurrences (Godwin et al., 1988). The Shale Curve of Godwin and Sinclair (1982) is shown for reference.

and $^{208}\text{Pb}/^{206}\text{Pb}$ ratios in this study, and four analyses of pyrite from the Hyland gold occurrence, which yielded the most radiogenic lead isotopic compositions. The majority of analyses ($n=9$) yield narrow ranges of $^{206}\text{Pb}/^{204}\text{Pb}$, $^{207}\text{Pb}/^{204}\text{Pb}$, $^{208}\text{Pb}/^{204}\text{Pb}$, $^{207}\text{Pb}/^{206}\text{Pb}$, and $^{208}\text{Pb}/^{206}\text{Pb}$ ratios with values of 19.396 to 19.615, 15.711 to 15.904, 39.391 to 40.039, 0.806 to 0.811, and 2.024 to 2.041, respectively.

DISCUSSION

The feldspar lead isotopic compositions are highly radiogenic and plot above the Shale Curve of Godwin and Sinclair (1982), which indicates that the intrusions are largely, if not entirely, the product of partial melting of Selwyn Basin-like sedimentary rocks (see Heffernan, 2004, for further discussion). Lead isotopic compositions of most sulphide minerals from occurrences proximal to the

plutons are very similar to feldspar lead isotopic compositions from the plutons themselves. This is consistent with the metals having been derived mainly from the plutons.

Sulphide lead isotopic compositions from the past producing Sa Dena Hes zinc-lead-silver skarn deposit plot within the cluster of lead analyses for feldspars from Cretaceous intrusions and for associated sulphide minerals. Rare felsic and andesitic dykes are known to be associated with, and possibly related to, mineralization at the mine but have not been dated directly. The similarity in lead isotopic compositions suggests that the deposit is also mid-Cretaceous in age and probably related to a Cretaceous intrusion that is not exposed in the area.

Lead isotopic compositions from the Quartz Lake (McMillan) occurrence in the southeastern part of the study area and from the Hyland gold occurrence (Fig. 2),

a gold-rich, base metal poor deposit located near the Quartz Lake occurrence, are much more radiogenic than any of the other sulphide minerals or feldspars from the area. The Hyland gold occurrence may represent a distal style of intrusion-related, structurally controlled disseminated gold mineralization, whereas the Quartz Lake deposit consists of massive sulphide replacement bodies. The similar lead isotopic compositions from these occurrences suggest similar sources for the metals; however, the measured lead isotopic compositions are very different from that of any of the Cretaceous intrusions in the study area. The implications of this are uncertain. It could indicate that: (1) the metals in the Quartz Lake and Hyland deposits were derived from an unidentified intrusive phase that is much more radiogenic than any recognized thus far in the study area; or (2) the metals were derived mainly from sedimentary sources and are completely unrelated to the plutons; or (3) the lead in these deposits represents a mixture of lead from igneous and sedimentary sources. The lead isotopic compositions of sulphide minerals from epigenetic occurrences sampled in this study are very different from typical SEDEX-type lead-zinc occurrences in the Selwyn Basin (Fig. 3), and thus indicates that these occurrences do not represent remobilized SEDEX-type mineralization.

CONCLUSIONS

The primary goal of this study was to compare and contrast the lead isotopic compositions of feldspars from various intrusions and sulphides from associated precious- and base-metal deposits and occurrences within the southeastern TGP in order to investigate possible linkages between magmatism and mineralization. Results from this study indicate that: (1) the metals in many mineral deposits and prospects in the region are mostly derived from the mid-Cretaceous TGP intrusions; (2) the Sa Dena Hes deposit is broadly mid-Cretaceous in age; and (3) metals in apparently distal styles of intrusion-related gold mineralization in this region are not entirely derived from magmatic sources. In an area with such voluminous magmatism and few mineral deposits, these results also serve to highlight the exploration potential throughout the study area.

ACKNOWLEDGEMENTS

This work was completed as part of the author's MSc thesis at the University of British Columbia in conjunction with the Pacific Centre for Isotopic and Geochemical Research (PCIGR) and the Mineral Deposit Research Unit (MDRU). Funding and support for this project were provided by an NSERC Research Grant (to J.K. Mortensen), an NSERC Collaborative Research and Development Grant (to J.K. Mortensen and the MDRU), the Yukon Geological Survey, Hudson Bay Exploration and Development Co. Ltd., and a Hugh E. McKinstry Grant (to R.S. Heffernan). Thanks to Dave Hladky and StrataGold Corporation for providing samples from Hyland. Also, thanks goes to Dick Tosdal of the MDRU for providing a critical review of this paper.

REFERENCES

- Deklerk, R. and Traynor, S., 2004 (compilers.). Yukon MINFILE – A database of mineral occurrences. Yukon Geological Survey, CD-ROM.
- Godwin, C.I. and Sinclair, A.J., 1982. Average lead isotope growth curves for shale-hosted zinc-lead deposits, Canadian Cordillera. *Economic Geology*, vol. 77, p. 208-211.
- Godwin C.I., Gabites, J.E. and Andrew, A., 1988. Leadtable: A galena lead isotope database for the Canadian Cordillera. *In: British Columbia Ministry of Energy and Mines and Petroleum Resources Paper 1988-4*, 214 p.
- Gordey, S.P. and Anderson, R.G. 1993. Evolution of the northern Cordillera Miogeocline, Nahanni Map Area (1051), Yukon and Northwest Territories. *Geological Survey of Canada Memoir 428*, 214 p.
- Gordey, S.P. and Makepeace, A.J. (compilers), 2001. *Bedrock Geology, Yukon Territory. In: Geological Survey of Canada, Open File 3754 and Exploration and Geological Services Division, Yukon Region, Indian and Northern Affairs Canada, Open File 2001-1*, 1:1 000 000 scale.
- Hart, C.J.R., McCoy, D.T., Goldfarb, R.J., Smith, M., Roberts, P., Hulstein, R., Bakke, A.A. and Bundtzen, T.K., 2002. Geology, exploration and discovery in the Tintina Gold Province, Alaska and Yukon. *In: Society of Economic Geologists Special Publication 9, Integrated Methods for Discovery: Global Exploration in the 21st Century*, p. 241-274.

- Heffernan, R.S., 2004. Temporal, geochemical, isotopic, and metallogenic studies of mid-Cretaceous magmatism in the Tintina Gold Province, southeastern Yukon and southwestern Northwest Territories, Canada. Unpublished MSc thesis, University of British Columbia, British Columbia, Canada, 83 p.
- Lang, J.R. and Baker, T., 2001. Intrusion-related gold systems: the present level of understanding. *Mineralium Deposita*, vol. 36, no. 6, p. 477-489.
- Lang, J.R. (ed.), 2000. Regional and system-scale controls on the formation of copper and/or gold magmatic-hydrothermal mineralization: Final Report, Mineral Deposit Research Unit Special Publication no. 2, 115 p.
- Mortensen, J.K., Hart, C.J.R., Murphy, D.C. and Heffernan, S., 2000. Temporal evolution of Early and mid-Cretaceous magmatism in the Tintina Gold Belt. *In: The Tintina Gold Belt: Concepts, Exploration and Discoveries*, British Columbia and Yukon Chamber of Mines, Special Volume 2, p. 49-58.
- Thompson, J.F.H., Sillitoe, R.H., Baker, T., Lang, J.R. and Mortensen, J.K., 1999. Intrusion-related gold deposits associated with tungsten-tin provinces. *Mineralium Deposita*, vol. 34, no. 4, p. 323-334.
- Thirwall, M.F., 2000. Inter-laboratory and other errors in Pb isotope analyses investigated using a ^{207}Pb - ^{204}Pb double spike. *Chemical Geology*, vol. 163, p. 299-322.